METTL3 Facilitates Colorectal Carcinoma Progression via Regulating m6A-CRB3-Hippo Axis

Feng Liu
Shanghai University of Traditional Chinese Medicine
Xiaoli Xiao
Shanghai University of Traditional Chinese Medicine
Jiashu Pan
Shanghai University of Traditional Chinese Medicine
Ruohui Xu
Shanghai University of Traditional Chinese Medicine
Liang Dai
Shanghai University of Traditional Chinese Medicine
Mingzhe Zhu
Shanghai University of Traditional Chinese Medicine
Hanchen Xu
Shanghai University of Traditional Chinese Medicine
Yangxian Xu
Shanghai University of Traditional Chinese Medicine
Aiguang Zhao
Shanghai University of Traditional Chinese Medicine
Wenjun Zhou
Shanghai University of Traditional Chinese Medicine
Yanqi Dang (dangyanqi9022@126.com)
Shanghai University of Traditional Chinese Medicine
Guang Ji
Shanghai University of Traditional Chinese Medicine

Research

Keywords: Colorectal carcinoma, RNA N6-methyladnosine, Methyltransferase-like 3, Crumbs3, Hippo pathway

Posted Date: June 17th, 2021

DOI: https://doi.org/10.21203/rs.3.rs-608084/v1

Abstract

Background

Colorectal carcinoma (CRC) is the third most common cancer and the second most common cause of cancer-related death worldwide. RNA N6-methyladnosine (m6A) and methyltransferase-like 3 (METTL3) play an important role in cancer. However, the roles of m6A and METTL3 in CRC progression are still elusive.

Methods

Adenoma and CRC samples were applied to detect m6A and METTL3 levels, and tissue microarrays were performed to evaluate their associations with survival of CRC patients. The biological functions of METTL3 were investigated by CCK8, wound healing and transwell assays. M6A epitranscriptomic microarray, RNA stability and luciferase reporter assays were performed to explore the mechanism of METTL3 in CRC.

Results

m6A and METTL3 levels were significantly upregulated in both adenoma and CRC tissues, and the CRC patients with high m6A or METTL3 level had both shorter overall survival. METTL3 knockdown markedly inhibited the proliferation, migration and invasion of CRC cells. M6A epitranscriptomic microarray revealed that the cell polarity regulator Crumbs3 (CRB3) was the downstream target of METTL3. METTL3 knockdown markedly inhibited the degradation of CRB3 mRNA to increase the CRB3 expression. In addition, CRB3 level was also markedly reduced in both adenoma and CRC tissues, and the CRC patients with high CRB3 level had higher overall survival and disease free survival. CRB3 knockdown significantly promoted the proliferation, migration and invasion of CRC cells. Finally, CRB3 knockdown inhibited Hippo pathway, and increased nuclear localization of YAP.

Conclusions

The m6A and METTL3 levels were significantly increased in both adenoma and CRC tissues. The CRC patients with high m6A or METTL3 levels had shorter overall survival. Mechanistically, METTL3 regulated the initiation and progression of CRC via regulating m6A-CRB3-Hippo pathway.

Background

Colorectal carcinoma (CRC) is the third most common cancer and the second most common cause of cancer-related death worldwide [1]. Due to tumor metastasis and other complications, the mortality rate

of CRC remains high. Therefore, it is urgent to elucidate the molecular mechanism and effective therapeutic targets of CRC.

RNA N6-methyladnosine (m6A) is the most common and abundant RNA modification in eukaryotes [2, 3]. M6A modification is mainly mediated by the m6A methyltransferases, demethylases and reader proteins. The m6A methyltransferases mainly included methyltransferase-like 3 (METTL3) [4], methyltransferase-like 14 (METTL14) [5], and Wilms tumor 1 associated protein (WTAP) [6], RNA binding motif protein 15 [7], and vir like m6A methyltransferase associated [8]. The m6A demethylases mainly included fat-mass and obesity-associated protein (FTO) [9], alkylation repair homolog protein 5 (ALKBH5) [10]. The reader proteins mainly included YTH domain-containing family protein 1/2/3 (YTHDF1/2/3), YTH domain containing 1/2, and insulin-like growth factor 2 mRNA binding proteins 1/2/3 and heterogeneous nuclear ribonucleoprotein family [11–13]. Some studies have proved that m6A modification plays a critical role in cancer [9, 14]. METTL3 could regulate the progression of cancer, including bladder cancer [15, 16], gastric cancer [17, 18], cervical cancer [19], hepatocellular carcinoma [14]. METTL14 could regulate hepatocellular carcinoma and pancreatic cancer progression [20, 21]. FTO plays an important role in oral squamous cell carcinoma [22], hepatocellular carcinoma [23], bladder cancer [24], acute myeloid leukemia [9, 25]. Although studies also showed that m6A modification plays a critical role in CRC [4, 12], the function and regulatory mechanism of m6A in CRC progression are still largely elusive.

In this study, we firstly verified the m6A level in both adenoma, which was precancerous lesions of CRC, and CRC tissues, and further demonstrated the function of METTL3 in CRC progression. Moreover, we identified crumbs3 (CRB3) as a downstream target of METTL3, and proved the function of CRB3 in CRC. Finally, we found that CRB3 regulated CRC progression by Hippo pathway. Therefore, our findings elucidated the roles of m6A and METTL3 and provided a new treatment strategy against CRC.

Materials And Methods

Clinical tissue specimens

Thirty CRC, thirty adenoma and thirty adjacent normal tissues (normal) were obtained during surgery in the Longhua Hospital affiliated with Shanghai University of Traditional Chinese Medicine. The diagnosis of CRC and adenoma was confirmed based on pathological evidence. Tissues were snap-frozen in liquid nitrogen and stored at -80°C before detection. The study was approved by the Ethics Committee of Longhua Hospital (2019LCSY020), and informed consent was obtained from all participants.

RNA m6A quantification assay

M6A level was assayed using an RNA m6A quantification kit (ab185912, abcam, USA) according to previous study [26]. In brief, 200ng RNA was incubated for 60 min with the capture antibody; and then the detection antibody and enhancer solution were added. Finally, samples were incubated with developer solution for 10 min. The absorbance was detected at a wavelength of 450 nm.

Immunohistochemistry

Tissue samples from the normal, adenoma, and CRC groups were fixed, and then cut into 4-μm sections for immunohistochemistry (IHC). Tissue microarrays (TMAs) were obtained from Shanghai Outdo Biotech Co., Ltd (Shanghai, China), and IHC was performed. In brief, samples were incubated with the m6A antibody (56593, CST, USA), and METTL3 antibody (ab195352, Abcam, USA) overnight at 4°C. Subsequently, the secondary antibodies were incubated for 1 h at 37◦C. Finally, samples were stained, and then imaged. The scores of IHC were performed.

Immunofluorescence

The m6A antibody (56593, CST, USA), METTL3 antibody (ab195352, Abcam, USA), and CRB3 antibody (PA5-53092, Thermo Fisher, USA) were obtained. Samples were incubated with the m6A antibody, METTL3 antibody, and CRB3 antibody overnight at 4◦C. Subsequently, the secondary antibodies conjugated with Alexa Fluor were incubated for 1 h at 37◦C. Finally, samples were stained, and then imaged.

Cell culture and transfection

Normal colon cells (FHC) and CRC cells (HCT116, HT29, SW480 and SW620) (Shanghai Cell Bank, shanghai, China) were cultured in DMEM supplemented with 10% FBS and penicillin/streptomycin (100 U/mL) in an incubator with 5% CO_2 at 37°C. In addition, 293T cells obtained from ATCC were cultured in RPMI Medium 1640 with 10% fetal bovine serum and penicillin/streptomycin (100 U/mL) (Gibco, Carlsbad, USA). METTL3 short hairpin RNA plasmid (sh-METTL3), CRB3 short hairpin RNA plasmid (sh-CRB3) or negative control (sh-NC) (Genomeditech, China) were transfected using FuGene® HD transfection reagent (Promega, USA) according to a previous study [27].

CCK8 assay

After transfection, HCT116 and SW620 cells were seeded into 96-well plates at a concentration of 1×10^4 cells and cultured for 0, 24, 48 and 72 h. Then, 10 μl CCK8 was added to each well. After incubation at 37°C for 1 h, the absorbance value was detected at 450 nm.

Wound healing assay

After transfection, HCT116 and SW620 cells were seeded in a six-well dish with a culture insert (Ibidi, Germany) at a concentration of 3×10^4 cells. After 24 h, the culture insert was removed, and the cells were washed twice with phosphate buffer. Then 2ml serum-free medium was added to each dish for 48 h. Images were captured, and the wound area was measured using ImageJ software (National Institutes of Health, USA).

Transwell assay

Six-well plates with 8-μm chambers (Corning, USA) were used to assess cellular migration (without Matrigel) or invasion (with Matrigel). Briefly, transfected HCT116 and SW620 cells were seeded in 6-well plates at a concentration of 1×10^5 cells. 200μl serum-free medium was added to the upper chamber, and 600 μl of medium with 30% fetal bovine serum was added to the lower chamber for 48 h. Then, the cells

were fixed with 4% paraformaldehyde for 30 min and stained with 0.1% crystal violet solution for 15 min. Five fields were randomly selected to calculate the number of migrating or invading cells.

Quantitative real-time PCR

Total RNA was extracted using TRIzol reagent (Ambion, USA). cDNA was synthesized using an EVM-MLV reverse transcription kit (Aikeri Biotech, Hunan, China). The amplification reaction was performed using the SYBR-Green qPCR kit (Thermo Fisher Scientific, MA, USA). Gene expression was normalized using β-actin. The primers were listed in Additional file 3 Table S1.

Western blotting

Cells were collected and lysed. Protein concentration was determined. The protein was separated and transferred to a PVDF membrane followed by incubation with 5% milk at room temperature for 1 h. The membrane was incubated at 4°C overnight with the following antibodies as indicated: METTL3 (86132, CST, USA), CRB3 (NBP1-98328, Novus Biologicals, USA), YTHDF2 (80014, CST, USA), MST1 (3682, CST, USA), phospho-MST1 (49332, CST, USA), SAV1 (13301, CST, USA), LATS1 (3477, CST, USA), phospho-LATS1 (8654, CST, USA), MOB1 (13730, CST, USA), phospho-MOB1 (8699, CST, USA), YAP (4912, CST, USA), phospho-YAP (13008, CST, USA), Histone (4499S, CST, USA), and β-actin (4970s, CST, USA). Then, the secondary antibody was added and incubated at room temperature for 1 h, and protein expression was observed using a chemiluminescence gel imaging system (Tanon 5200, China).

Human m6A Epitranscriptomic microarray analysis

Total RNA was quantified using the NanoDrop ND-1000. The sample preparation and microarray hybridization were performed based on the Arraystar's standard protocols. Briefly, the total RNAs were immunoprecipitated with anti- m6A antibody. The modified RNAs were eluted from the immunoprecipitated magnetic beads as the "IP". The unmodified RNAs were recovered from the supernatant as "Sup". The "IP" and "Sup" RNAs were labeled with Cy5 and Cy3 respectively using Arraystar Super RNA Labeling Kit. The RNAs were combined together and hybridized onto Arraystar Human m6A Epitranscriptomic Microarray (8x60K, Arraystar). After washing the slides, the arrays were scanned by an Agilent Scanner G2505C.

Data Processing and Analysis

Agilent Feature Extraction software was used to analyze acquired array images. Raw intensities of IP (Cy5-labelled) and Sup (Cy3-labelled) were normalized. After normalization, the probe signals were retained for further "m6A methylation level" and "m6A quantity" analysis. "m6A methylation level" was calculated for the percentage of modification based on the IP (Cy5-labelled) and Sup (Cy3-labelled) normalized intensities. "m6A quantity" was calculated for the m6A methylation amount based on the IP (Cy5-labelled) normalized intensities. Differentially m6A-methylated RNAs between two comparison groups were identified by filtering with the thresholds of fold change (FC) > 1.5 and P value < 0.05.

RNA stability assay

HCT116 cells were seeded in 6-well plates for 24h, and then treated with 5 μg/mL actinomycin D (MCE, USA) at the 0, 2, 4, 8, 24 h. Total RNA was then isolated by TRIzol (Ambion, USA) and analyzed by qPCR. The mRNA expression for each group at the indicated time was calculated and normalized by β-Actin.

Double luciferase reporter assay

Here, 293T cells were seeded in 24-well plates and transfected using FuGene® HD transfection reagent (Promega, USA) according to a previous study [28]. Briefly, 293T cells were transfected with CRB3 wild type (CRB3-WT; Genomeditech, China) or CRB3 mutant (CRB3-Mut; Genomeditech, China) plasmid with or without METTL3 knockdown for 6 h. Luciferase activity was detected using the dual-luciferase reporter system (Promega, USA).

Statistical analysis

Statistical analysis was conducted using SPSS 24.0 software. Data were assessed using a two-tailed Student's t-test. Survival curves were generated using the Kaplan–Meier method and compared using the log-rank test. Survival data were performed by univariate and multivariate Cox regression analyses. The distribution differences of the variables were analyzed by the Pearson's chi-square test. $P < 0.05$ was considered statistically significant.

Results

M6A level was markedly increased in both adenoma and CRC, and associated with poor prognosis

A recent study has indicated that approximately 85% of CRCs may be transformed from adenomas[29], so we firstly checked the level of m6A in both adenoma and CRC tissues. The results showed that the levels of m6A were markedly increased between both adenoma and CRC groups compared with the normal group (Fig. 1a-c). TMA was performed to explore the correlation between m6A with survival in CRC patients. The results indicated that the level of m6A was also markedly increased in the CRC group compared with the normal group (Fig. 1d-e). And the CRC patients with high m6A level had shorter overall survival (Fig. 1f, Additional file 3: Table S2), which suggests that m6A level might serve as a prognostic marker of CRC.

METTL3 was markedly increased in both adenoma and CRC, and associated with poor prognosis

M6A modification is regulated by RNA methyltransferase and demethylase, so we further detected the expression of methyltransferase (METTL3, METTL14 and WTAP) and demethylase (FTO and ALKBH5) in both adenoma and CRC. The results showed that expression of METTL3 was significantly increased in both the adenoma and CRC groups compared with the normal group (Fig. 2a-c), consistent with the results in the database (Additional file 1: Fig. S1A). METTL14 was significantly increased in only

adenoma, not in CRC (Additional file 1: Fig. S1B). FTO was significantly decreased in only adenoma, not in CRC (Additional file 1: Fig. S1C). WTAP and ALKBH5 had no difference among three groups (Additional file 1: Figure S1D and 1E). The mRNA and protein levels of METTL3 were also markedly increased in CRC cells (Fig. 2d-e). To explore the correlation between METTL3 with survival of CRC patients, TMA was performed. The results indicated that the level of METTL3 was also markedly increased in the CRC group compared with the normal group (Fig. 2f-g). And the CRC patients with high METTL3 level had shorter overall survival (Fig. 2h, Additional file 3: Table S3), which suggests that METTL3 level might also serve as a prognostic marker of CRC.

METTL3 drives CRC proliferation and invasion

To investigate the function of METTL3 in CRC, the knockdown of METTL3 was established in HCT116 and SW620 cells (Fig. 3a). The knockdown of METTL3 significantly inhibited the proliferation of HCT116 and SW620 cells (Fig. 3b). Transwell assays showed that METTL3 knockdown markedly inhibited migration and invasion of HCT116 and SW620 cells (Fig. 3c-d), and METTL3 knockdown also significantly decreased the migration speed of HCT116 and SW620 cells (Fig. 3e-f).

CRB3 was regulated by METTL3-mediated m6A modification

To investigate the potential mechanism of METTL3 in CRC progression, the epitranscriptomic microarray was performed, and data were analyzed. In the m6A methylation level, 363 differentially m6A methylated sites (DMS) were identified, including 353 upregulated DMS and 10 downregulated DMS (Fig. 4a, Additional file 4). And further analysis found that these 363 DMS belonged to 349 differentially m6A methylated genes (DMG), including 341 upregulated DMG and 8 downregulated DMG (Fig. 4b). In the m6A quantity level, 248 DMS were identified, including 191 upregulated DMS and 57 downregulated DMS (Fig. 4c, Additional file 5). And further analysis found that these 248 DMS belonged to 224 DMG, including 175 upregulated DMG and 49 downregulated DMG (Fig. 4d). Subsequently, the main functions were identified using GO and KEGG, including DNA binding, RNA polymerase II transcription factor activity, Toll-like receptor binding, beta-Alanine metabolism, alpha-Linolenic acid metabolism, Nicotinate and nicotinamide metabolism (Fig. 4e-h).

Seven overlapping DMG between the m6A methylation level and quantity level were filtered by a Venn diagram (Fig. 5a), and qPCR analysis indicated that CRB3 level was markedly increased after METTL3 knockdown (Fig. 5b-c). The result of The Cancer Genome Atlas (TCGA) database revealed that CRB3 level was markedly downregulated in the CRC group (Additional file 2: Fig. S2B). The survival analysis indicated that the CRC patients with high CRB3 levels had higher overall survival and disease free survival (Additional file 2: Fig. S2C). Although METTL3 knockdown also promoted bridging integrator 1 (BIN1) level, the BIN1 expression was markedly increased in the CRC group (Additional file 2: Fig. S2A and 2D). The survival analysis indicated that there was no correlation between BIN1 levels and CRC patient survival (Additional file 2: Fig. S2E). In addition, luciferase reporters were performed to determine the

effect of m6A modification on CRB3 expression. For the mutant form of CRB3, the adenosine bases in m6A consensus sequences (GGAC) were replaced by cytosine, thus m6A modification was abolished. The results showed that transcriptional level of wild-type CRB3 significantly increased after METTL3 knockdown, but not the mutation (Fig. 5d). RNA stability assay revealed that METTL3 knockdown markedly inhibited the degradation of CRB3 mRNA (Fig. 5e). Moreover, METTL3 mRNA expression in CRC tissues was negatively associated with CRB3 levels according to TCGA database (Fig. 5f). Recent studies have reported that YTHDF2 could target mRNAs via recognizing m6A motif in CRC [5, 12], so we explored the effect of YTHDF2 on CRB3. The results showed that expression of YTHDF2 was also significantly increased in the adenoma and CRC tissues (Fig. 5g), and YTHDF2 knockdown markedly increased the level of CRB3 (Fig. 5h). The results showed that METTL3 regulated the expression of CRB3 by an m6A-dependent manner.

CRB3 inhibited CRC proliferation and invasion

Our results also showed that CRB3 level was markedly decreased in the adenoma and CRC groups, which was consistent with the TCGA database (Fig. 6a-b, Additional file 2: Fig. S2B). To further investigate the function of CRB3 in CRC, CRB3 knockdown was established in HCT116 and SW620 cells. The knockdown of CRB3 significantly promoted the proliferation of HCT116 and SW620 cells (Fig. 6c). Transwell assays showed that CRB3 knockdown markedly increased migration and invasion of HCT116 and SW620 cells (Fig. 6d-e), and CRB3 knockdown also significantly increased the migration speed of HCT116 and SW620 cells (Fig. 6f-g). The results fully proved that CRB3 regulated CRC progression.

CRB3 inhibited CRC progression by regulating Hippo pathway

Previous studies have proved that CRB3 could regulate Hippo pathway [30, 31]. In the present study, we found that CRB3 knockdown decreased MST1, LATS1, MOB1 and YAP phosphorylation levels, and also decreased SAV1 level in HCT116 and SW620 cells (Fig. 7a-b). In addition, CRB3 knockdown markedly increased YAP protein level (Fig. 7a-b). Studies have proved that YAP enters the nucleus and acts as an oncogene. So we also detected the level of YAP in the nucleus, and results showed that CRB3 knockdown also markedly increased YAP protein level in the nucleus of HCT116 and SW620 cells (Fig. 7c-d). The results indicated that CRB3 could regulate CRC progression by Hippo pathway.

Discussion

As a malignant tumor, the incidence of CRC has recently increased. Although the five-year survival rate of CRC patients is 65% [32], the five-year survival rate of patients with advanced-stage CRC is very low. Therefore, it is urgent to develop techniques for the treatment strategy of CRC, which would improve patient survival [27]. Studies have indicated that m6A modification plays a critical role in CRC [4, 5, 12, 33]. But the change of m6A in both adenoma and CRC are still unknown. In addition, the relationship between m6A level and survival of CRC patients is also unknown. In this study, we first found that m6A

level was significantly increased in both adenoma and CRC tissues, indicating that m6A modification could be involved in the adenoma-CRC process. Further studies indicated that the CRC patients with high m6A level had shorter overall survival, which suggests that m6A level might serve as a prognostic marker of CRC.

M6A modification is mainly mediated by the m6A methyltransferases, demethylases and reader proteins, and regulates pre-mRNA splicing, miRNA processing, translation and mRNA decay [34]. In this study, we first found that the expression of METTL3 was significantly increased in both adenoma and CRC, showing that METTL3 could be involved in the initiation and progression of CRC. And the CRC patients with high METTL3 level had shorter overall survival, which suggests that METTL3 might also serve as a prognostic marker of CRC. The result was consistent with a previous study [4, 35]. Then we further verified the function of METTL3 in CRC. METTL3 knockdown inhibited the proliferation of HCT116 and SW620 cells, and also markedly inhibited migration and invasion of HCT116 and SW620 cells. These results indicated that METTL3 acted as an oncogene to promote the progression of CRC. Previous studies also proved that METTL3 plays an important role in a variety of cancers. METTL3 could regulate MALAT1 stabilization via m6A modification, and activate NF-κB activity to promote the malignant progression of glioma [36]. METTL3 increased miR-1246 level via the m6A modification, thus to promote non-small cell lung cancer progression [37]. Moreover, METTL3 regulated m6A modification of SPHK2 to contribute the progression of gastric cancer [38]. These findings fully proved the role of METTL3 in cancers, including CRC. Therefore, METTL3 could act as a new treatment target for cancers.

According to m6A Epitranscriptomic microarray analysis, we found that CRB3 might be the downstream target of METTL3. METTL3 knockdown markedly reduced the m6A level of CRB3 and increased the CRB3 expression. Previous studies have found that the m6A consensus sequences are GGAC [5]. Our study found that METTL3 knockdown increased the transcriptional level of CRB3. When the adenosine bases of GGAC in CRB3 were replaced by cytosine, thus the transcriptional level of CRB3 was no change. In addition, further study found that METTL3 knockdown markedly inhibited the degradation of CRB3 mRNA. These results indicated that CRB3 was a target of METTL3 in CRC. CRB3 is a protein of cell polarity, and associated with contact inhibition [39]. Previous studies proved that CRB3 played an important role in cancer, including CRC [30, 40, 41]. In present study, we found that CRB3 level was markedly reduced in both adenoma and CRC, and the CRC patients with high CRB3 levels had higher overall survival and disease free survival. CRB3 knockdown significantly promoted the proliferation, migration and invasion of HCT116 and SW620 cells. These results indicated that CRB3 regulated CRC progression.

The depletion of CRB3 could regulate hippo pathway and lead to increased nuclear localization of YAP/TAZ [30, 31, 42]. The hippo pathway plays a crucial role in regulating the CRC progression [43–46]. In present study, we found that CRB3 knockdown inhibited Hippo pathway, and increased nuclear localization of YAP, suggesting that CRB3 regulated the CRC progression by Hippo pathway. Finally, our study found that METTL3 facilitated CRC progression via regulating m6A-CRB3-Hippo pathway, which was a novel mechanism for regulating CRC. Nevertheless, although we proved the regulatory mechanism

of METTL3 in CRC,further studies would be needed. First, although previous study has found that selective first-in-class catalytic inhibitor of METTL3 (STM2457) could act as a strategy against acute myeloid leukaemia [47]. But so far, the inhibitor of METTL3 has been not found in the treatment of CRC, and further studies which find the inhibitor of METTL3 are needed. Second, although we found that m6A and METTL3 levels were markedly increased in both adenoma and CRC□the function in the adenoma-CRC transition are needed in future study.

Conclusion

In summary, we demonstrated that m6A and METTL3 levels were significantly increased in both adenoma and CRC. The CRC patients with high m6A or METTL3 level had shorter overall survival. Mechanistically, METTL3 regulates the initiation and maintenance of CRC via regulating m6A-CRB3-Hippo pathway. These findings provide a new perspective for targeted therapy of CRC.

Abbreviations

CRC: Colorectal carcinoma; m6A: N6-methyladnosine; METTL3: Methyltransferase-like 3; CRB3: Crumbs3; METTL14: Methyltransferase-like 14; WTAP: Wilms tumor 1 associated protein; FTO: Fat-mass and obesity-associated protein; ALKBH5: Alkylation repair homolog protein 5; YTHDF1/2/3: YTH domain-containing family protein 1/2/3; Normal: Adjacent normal tissues; IHC: Immunohistochemistry; TMA: Tissue microarrays; MeRIP-Qpcr: Methylated RNA immunoprecipitation-qPCR; DMS: Differentially m6A methylated sites; DMG: differentially m6A methylated genes; TCGA: The Cancer Genome Atlas; BIN1: Bridging integrator 1

Declarations

Acknowledgments

We thank KangChen Biotech (Shanghai, China) for the m6A Epitranscriptomic microarray service and Shanghai Outdo Biotech Co.,Ltd for TMA.

Authors' contributions

GJ and YD conceived, designed and supervised the study. YD, FL, and YX collected samples. FL, XX, JP, and RX performed the experiments, and YD, FL, XX, LD and MZ analyzed the data. YD and JP wrote the paper. AZ, WZ and HX edited and revised the paper. All authors reviewed and approved the final manuscript.

Funding

This work was supported by the National Natural Science Foundation of China (81804018 and 81620108030), the Key Project of Shanghai 3-year plan (ZY(2018-2020)CCCX-2002-01) and Shanghai

Rising-Star Program (21QA1409000).

Availability of data and material

The datasets used and/or analyzed during the current study are available from the corresponding author on reasonable request.

Ethics approval and consent to participate

This study was approved by the Ethics Committee of Longhua Hospital (2019LCSY020), and the informed consent was obtained from all participants.

Consent for publication

All authors have agreed to publish this manuscript

Competing interests

The authors declare that they have no competing interests.

References

1. Sung H, Ferlay J, Siegel RL, Laversanne M, Soerjomataram I, Jemal A, Bray F. Global Cancer Statistics 2020: GLOBOCAN Estimates of Incidence and Mortality Worldwide for 36 Cancers in 185 Countries. CA Cancer J Clin. 2021;71(3):209–49.
2. Meyer KD, Saletore Y, Zumbo P, Elemento O, Mason CE, Jaffrey SR. Comprehensive analysis of mRNA methylation reveals enrichment in 3' UTRs and near stop codons. Cell. 2012;149(7):1635–46.
3. Zhao BS, Roundtree IA, He C. Post-transcriptional gene regulation by mRNA modifications. Nat Rev Mol Cell Biol. 2017;18(1):31–42.
4. Li T, Hu PS, Zuo Z, Lin JF, Li X, Wu QN, Chen ZH, Zeng ZL, Wang F, Zheng J, et al. METTL3 facilitates tumor progression via an m(6)A-IGF2BP2-dependent mechanism in colorectal carcinoma. Mol Cancer. 2019;18(1):112.
5. Chen X, Xu M, Xu X, Zeng K, Liu X, Pan B, Li C, Sun L, Qin J, Xu T, et al. METTL14-mediated N6-methyladenosine modification of SOX4 mRNA inhibits tumor metastasis in colorectal cancer. Mol Cancer. 2020;19(1):106.
6. Selberg S, Blokhina D, Aatonen M, Koivisto P, Siltanen A, Mervaala E, Kankuri E, Karelson M. Discovery of Small Molecules that Activate RNA Methylation through Cooperative Binding to the METTL3-14-WTAP Complex Active Site. Cell Rep. 2019;26(13):3762–71 e3765.
7. Wang X, Tian L, Li Y, Wang J, Yan B, Yang L, Li Q, Zhao R, Liu M, Wang P, et al. RBM15 facilitates laryngeal squamous cell carcinoma progression by regulating TMBIM6 stability through IGF2BP3 dependent. J Exp Clin Cancer Res. 2021;40(1):80.

8. Barros-Silva D, Lobo J, Guimaraes-Teixeira C, Carneiro I, Oliveira J, Martens-Uzunova ES, Henrique R, Jeronimo C. **VIRMA-Dependent N6-Methyladenosine Modifications Regulate the Expression of Long Non-Coding RNAs CCAT1 and CCAT2 in Prostate Cancer**. *Cancers (Basel)* 2020, 12(4).
9. Li Z, Weng H, Su R, Weng X, Zuo Z, Li C, Huang H, Nachtergaele S, Dong L, Hu C, et al. FTO Plays an Oncogenic Role in Acute Myeloid Leukemia as a N(6)-Methyladenosine RNA Demethylase. Cancer Cell. 2017;31(1):127–41.
10. Zhang S, Zhao BS, Zhou A, Lin K, Zheng S, Lu Z, Chen Y, Sulman EP, Xie K, Bogler O, et al. m(6)A Demethylase ALKBH5 Maintains Tumorigenicity of Glioblastoma Stem-like Cells by Sustaining FOXM1 Expression and Cell Proliferation Program. Cancer Cell. 2017;31(4):591–606 e596.
11. Huang H, Weng H, Sun W, Qin X, Shi H, Wu H, Zhao BS, Mesquita A, Liu C, Yuan CL, et al. Recognition of RNA N(6)-methyladenosine by IGF2BP proteins enhances mRNA stability and translation. Nat Cell Biol. 2018;20(3):285–95.
12. Zhou D, Tang W, Xu Y, Xu Y, Xu B, Fu S, Wang Y, Chen F, Chen Y, Han Y, et al: **METTL3/YTHDF2 m6A axis accelerates colorectal carcinogenesis through epigenetically suppressing YPEL5**. *Mol Oncol* 2021.
13. Ma L, Zhang X, Yu K, Xu X, Chen T, Shi Y, Wang Y, Qiu S, Guo S, Cui J, et al. Targeting SLC3A2 subunit of system XC(-) is essential for m(6)A reader YTHDC2 to be an endogenous ferroptosis inducer in lung adenocarcinoma. Free Radic Biol Med. 2021;168:25–43.
14. Chen M, Wei L, Law CT, Tsang FH, Shen J, Cheng CL, Tsang LH, Ho DW, Chiu DK, Lee JM, et al: **RNA N6-methyladenosine methyltransferase-like 3 promotes liver cancer progression through YTHDF2-dependent posttranscriptional silencing of SOCS2**. *Hepatology* 2018, **67**(6):2254–2270.
15. Han J, Wang JZ, Yang X, Yu H, Zhou R, Lu HC, Yuan WB, Lu JC, Zhou ZJ, Lu Q, et al. METTL3 promote tumor proliferation of bladder cancer by accelerating pri-miR221/222 maturation in m6A-dependent manner. Mol Cancer. 2019;18(1):110.
16. Cheng M, Sheng L, Gao Q, Xiong Q, Zhang H, Wu M, Liang Y, Zhu F, Zhang Y, Zhang X, et al. The m(6)A methyltransferase METTL3 promotes bladder cancer progression via AFF4/NF-kappaB/MYC signaling network. Oncogene. 2019;38(19):3667–80.
17. Wang Q, Chen C, Ding Q, Zhao Y, Wang Z, Chen J, Jiang Z, Zhang Y, Xu G, Zhang J, et al. METTL3-mediated m(6)A modification of HDGF mRNA promotes gastric cancer progression and has prognostic significance. Gut. 2020;69(7):1193–205.
18. Yue B, Song C, Yang L, Cui R, Cheng X, Zhang Z, Zhao G. METTL3-mediated N6-methyladenosine modification is critical for epithelial-mesenchymal transition and metastasis of gastric cancer. Mol Cancer. 2019;18(1):142.
19. Wang Q, Guo X, Li L, Gao Z, Su X, Ji M, Liu J. N(6)-methyladenosine METTL3 promotes cervical cancer tumorigenesis and Warburg effect through YTHDF1/HK2 modification. Cell Death Dis. 2020;11(10):911.
20. Du L, Li Y, Kang M, Feng M, Ren Y, Dai H, Wang Y, Wang Y, Tang B. **USP48 is upregulated by Mettl14 to attenuate hepatocellular carcinoma via regulating SIRT6 stabilization**. *Cancer Res* 2021.

21. Chen S, Yang C, Wang ZW, Hu JF, Pan JJ, Liao CY, Zhang JQ, Chen JZ, Huang Y, Huang L, et al. CLK1/SRSF5 pathway induces aberrant exon skipping of METTL14 and Cyclin L2 and promotes growth and metastasis of pancreatic cancer. J Hematol Oncol. 2021;14(1):60.
22. Wang F, Liao Y, Zhang M, Zhu Y, Wang W, Cai H, Liang J, Song F, Hou C, Huang S, et al: **N6-methyladenosine demethyltransferase FTO-mediated autophagy in malignant development of oral squamous cell carcinoma**. *Oncogene* 2021.
23. Bian X, Shi D, Xing K, Zhou H, Lu L, Yu D, Wu W. AMD1 upregulates hepatocellular carcinoma cells stemness by FTO mediated mRNA demethylation. Clin Transl Med. 2021;11(3):e352.
24. Tao L, Mu X, Chen H, Jin D, Zhang R, Zhao Y, Fan J, Cao M, Zhou Z. FTO modifies the m6A level of MALAT and promotes bladder cancer progression. Clin Transl Med. 2021;11(2):e310.
25. Su R, Dong L, Li C, Nachtergaele S, Wunderlich M, Qing Y, Deng X, Wang Y, Weng X, Hu C, et al. R-2HG Exhibits Anti-tumor Activity by Targeting FTO/m(6)A/MYC/CEBPA Signaling. Cell. 2018;172(1–2):90–105. e123.
26. Dang Y, Xu J, Yang Y, Li C, Zhang Q, Zhou W, Zhang L, Ji G. Ling-gui-zhu-gan decoction alleviates hepatic steatosis through SOCS2 modification by N6-methyladenosine. Biomed Pharmacother. 2020;127:109976.
27. Dang Y, Hu D, Xu J, Li C, Tang Y, Yang Z, Liu Y, Zhou W, Zhang L, Xu H, et al. Comprehensive analysis of 5-hydroxymethylcytosine in zw10 kinetochore protein as a promising biomarker for screening and diagnosis of early colorectal cancer. Clin Transl Med. 2020;10(3):e125.
28. Dang Y, Xu J, Zhu M, Zhou W, Zhang L, Ji G. Gan-Jiang-Ling-Zhu decoction alleviates hepatic steatosis in rats by the miR-138-5p/CPT1B axis. Biomed Pharmacother. 2020;127:110127.
29. Strum WB. Colorectal Adenomas. N Engl J Med. 2016;374(11):1065–75.
30. Mao X, Li P, Wang Y, Liang Z, Liu J, Li J, Jiang Y, Bao G, Li L, Zhu B, et al. CRB3 regulates contact inhibition by activating the Hippo pathway in mammary epithelial cells. Cell Death Dis. 2017;8(1):e2546.
31. Fernando RN, Cotter L, Perrin-Tricaud C, Berthelot J, Bartolami S, Pereira JA, Gonzalez S, Suter U, Tricaud N. Optimal myelin elongation relies on YAP activation by axonal growth and inhibition by Crb3/Hippo pathway. Nat Commun. 2016;7:12186.
32. Burgers K, Moore C, Bednash L. Care of the Colorectal Cancer Survivor. Am Fam Physician. 2018;97(5):331–6.
33. Chen C, Yuan W, Zhou Q, Shao B, Guo Y, Wang W, Yang S, Guo Y, Zhao L, Dang Q, et al. N6-methyladenosine-induced circ1662 promotes metastasis of colorectal cancer by accelerating YAP1 nuclear localization. Theranostics. 2021;11(9):4298–315.
34. Ma JZ, Yang F, Zhou CC, Liu F, Yuan JH, Wang F, Wang TT, Xu QG, Zhou WP, Sun SH. METTL14 suppresses the metastatic potential of hepatocellular carcinoma by modulating N(6) -methyladenosine-dependent primary MicroRNA processing. Hepatology. 2017;65(2):529–43.
35. Chen H, Gao S, Liu W, Wong CC, Wu J, Wu J, Liu D, Gou H, Kang W, Zhai J, et al. RNA N(6)-Methyladenosine Methyltransferase METTL3 Facilitates Colorectal Cancer by Activating the m(6)A-

GLUT1-mTORC1 Axis and Is a Therapeutic Target. Gastroenterology. 2021;160(4):1284–300 e1216.

36. Chang YZ, Chai RC, Pang B, Chang X, An SY, Zhang KN, Jiang T, Wang YZ. METTL3 enhances the stability of MALAT1 with the assistance of HuR via m6A modification and activates NF-kappaB to promote the malignant progression of IDH-wildtype glioma. Cancer Lett. 2021;511:36–46.
37. Huang S, Luo S, Gong C, Liang L, Xiao Y, Li M, He J. MTTL3 upregulates microRNA-1246 to promote occurrence and progression of NSCLC via targeting paternally expressed gene 3. Mol Ther Nucleic Acids. 2021;24:542–53.
38. Huo FC, Zhu ZM, Zhu WT, Du QY, Liang J, Mou J. METTL3-mediated m(6)A methylation of SPHK2 promotes gastric cancer progression by targeting KLF2. Oncogene. 2021;40(16):2968–81.
39. Karp CM, Tan TT, Mathew R, Nelson D, Mukherjee C, Degenhardt K, Karantza-Wadsworth V, White E. Role of the polarity determinant crumbs in suppressing mammalian epithelial tumor progression. Cancer Res. 2008;68(11):4105–15.
40. Iioka H, Saito K, Kondo E. Crumbs3 regulates the expression of glycosphingolipids on the plasma membrane to promote colon cancer cell migration. Biochem Biophys Res Commun. 2019;519(2):287–93.
41. Li P, Feng C, Chen H, Jiang Y, Cao F, Liu J, Liu P. Elevated CRB3 expression suppresses breast cancer stemness by inhibiting beta-catenin signalling to restore tamoxifen sensitivity. J Cell Mol Med. 2018;22(7):3423–33.
42. Szymaniak AD, Mahoney JE, Cardoso WV, Varelas X. Crumbs3-Mediated Polarity Directs Airway Epithelial Cell Fate through the Hippo Pathway Effector Yap. Dev Cell. 2015;34(3):283–96.
43. Jin L, Chen Y, Cheng D, He Z, Shi X, Du B, Xi X, Gao Y, Guo Y. YAP inhibits autophagy and promotes progression of colorectal cancer via upregulating Bcl-2 expression. Cell Death Dis. 2021;12(5):457.
44. Shen H, Huang C, Wu J, Li J, Hu T, Wang Z, Zhang H, Shao Y, Fu Z. SCRIB Promotes Proliferation and Metastasis by Targeting Hippo/YAP Signalling in Colorectal Cancer. Front Cell Dev Biol. 2021;9:656359.
45. Tian C, Lang T, Qiu J, Han K, Zhou L, Min D, Zhang Z, Qi D. SKP1 promotes YAP-mediated colorectal cancer stemness via suppressing RASSF1. Cancer Cell Int. 2020;20(1):579.
46. Sun Z, Zhang Q, Yuan W, Li X, Chen C, Guo Y, Shao B, Dang Q, Zhou Q, Wang Q, et al. MiR-103a-3p promotes tumour glycolysis in colorectal cancer via hippo/YAP1/HIF1A axis. J Exp Clin Cancer Res. 2020;39(1):250.
47. Yankova E, Blackaby W, Albertella M, Rak J, De Braekeleer E, Tsagkogeorga G, Pilka ES, Aspris D, Leggate D, Hendrick AG, et al: **Small molecule inhibition of METTL3 as a strategy against myeloid leukaemia**. *Nature* 2021.

Figures

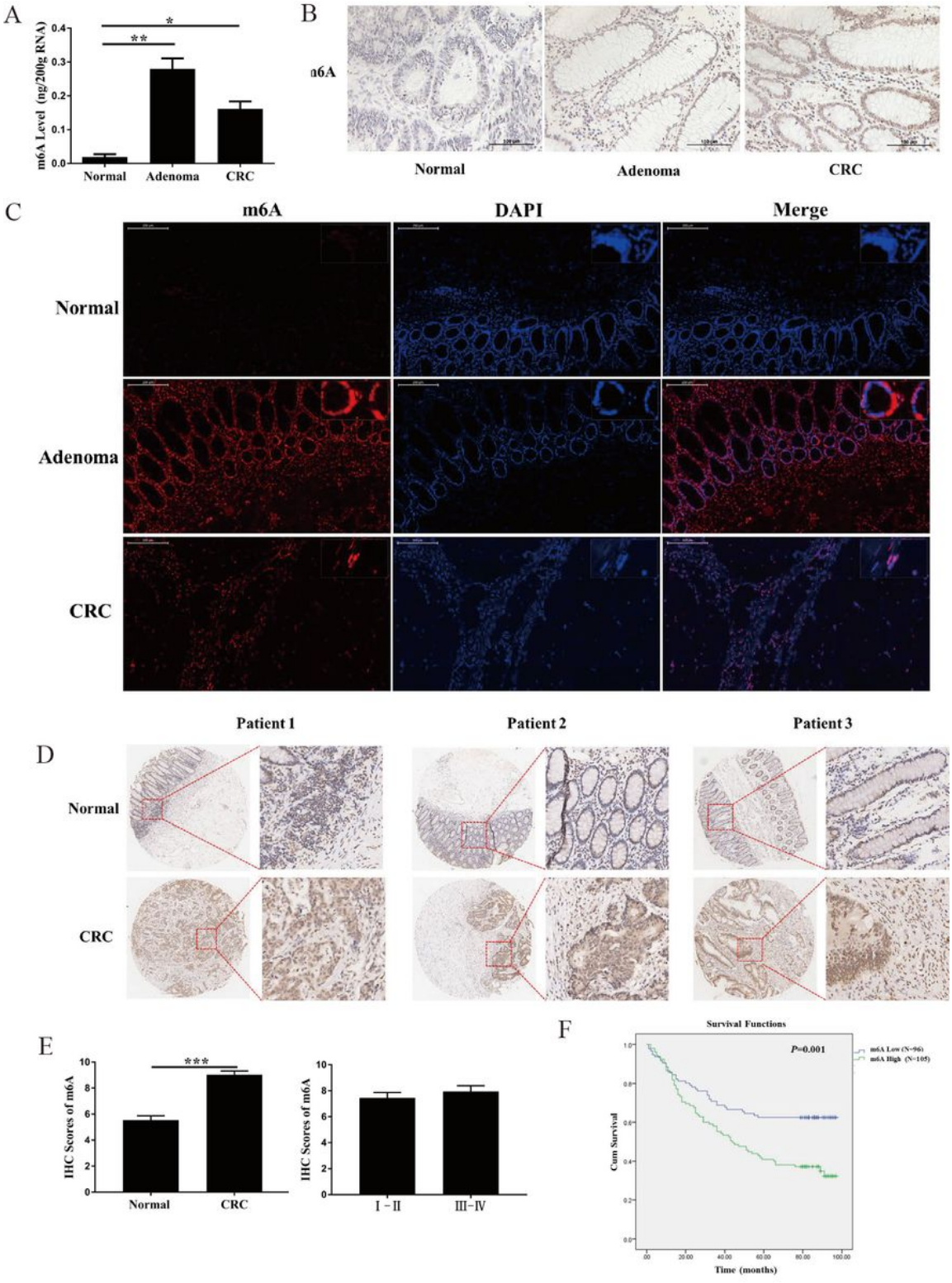

Figure 1

M6A level was markedly increased in both adenoma and CRC, and associated with poor prognosis. M6A levels in both adenoma and CRC were assayed by methylation quantification assay (a), Immunohistochemistry (b), and Immunofluorescence (c); (d) Representive images of IHC staining for m6A level from 201 CRC tissues and 159 normal tissues; (e) m6A IHC staining scores; (f) Kaplan-Meier

OS analysis of m6A expression in CRC patients. Data were presented as means ±SD. *P < 0.05, **P < 0.01, ***P < 0.001.

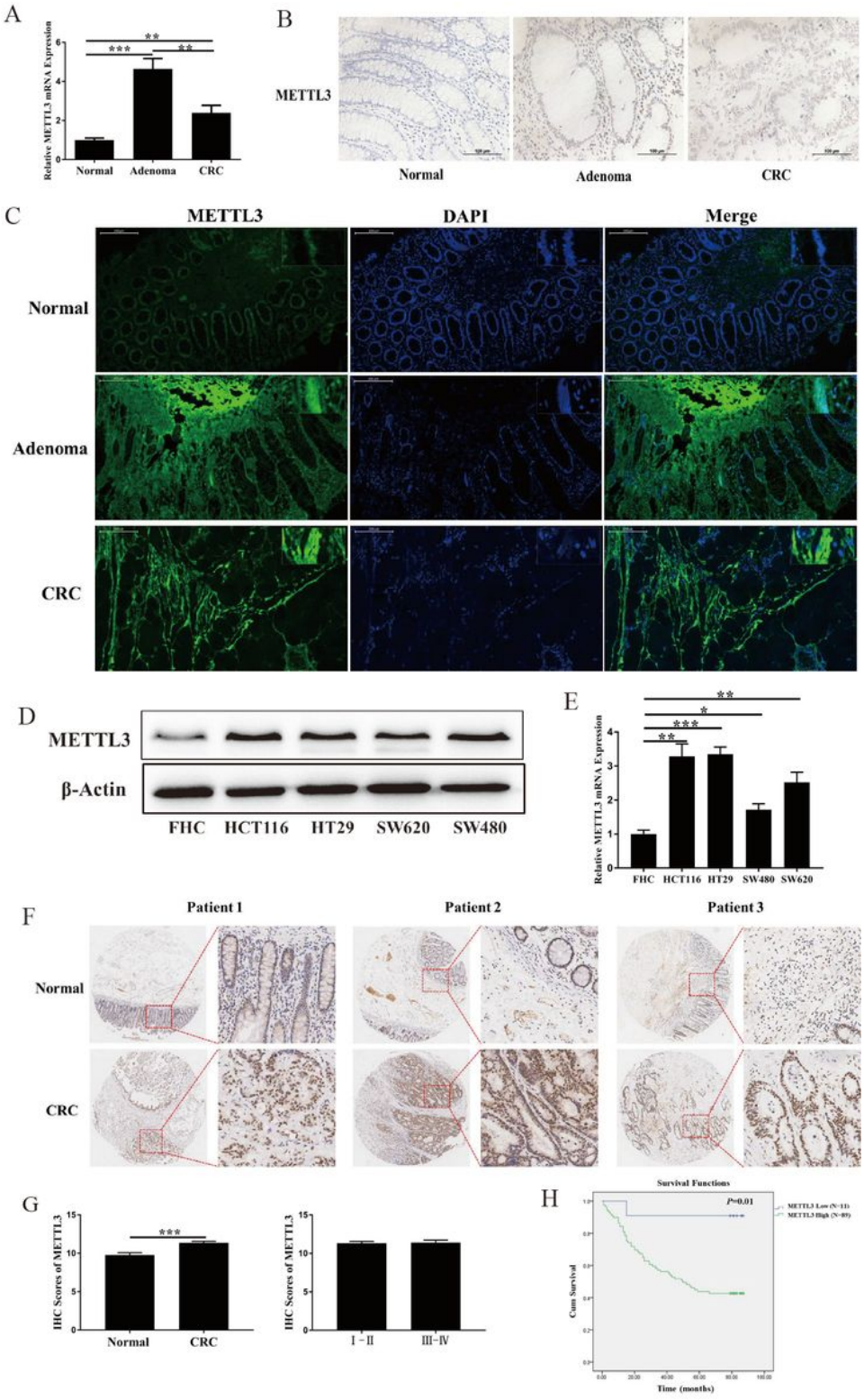

Figure 2

METTL3 was markedly increased in both adenoma and CRC, and associated with poor prognosis. METTL3 expression in both adenoma and CRC was assayed by qPCR (a), Immunohistochemistry (b), and Immunofluorescence (c); (d) METTL3 protein level in CRC cells was detected; (e) METTL3 mRNA level in

CRC cells was detected; (f) Representive images of IHC staining for METTL3 level from 100 CRC tissues and 80 normal tissues; (g) METTL3 IHC staining scores; (h) Kaplan-Meier OS analysis of METTL3 expression in CRC patients. Data were presented as means ±SD. *P < 0.05, **P < 0.01, ***P < 0.001.

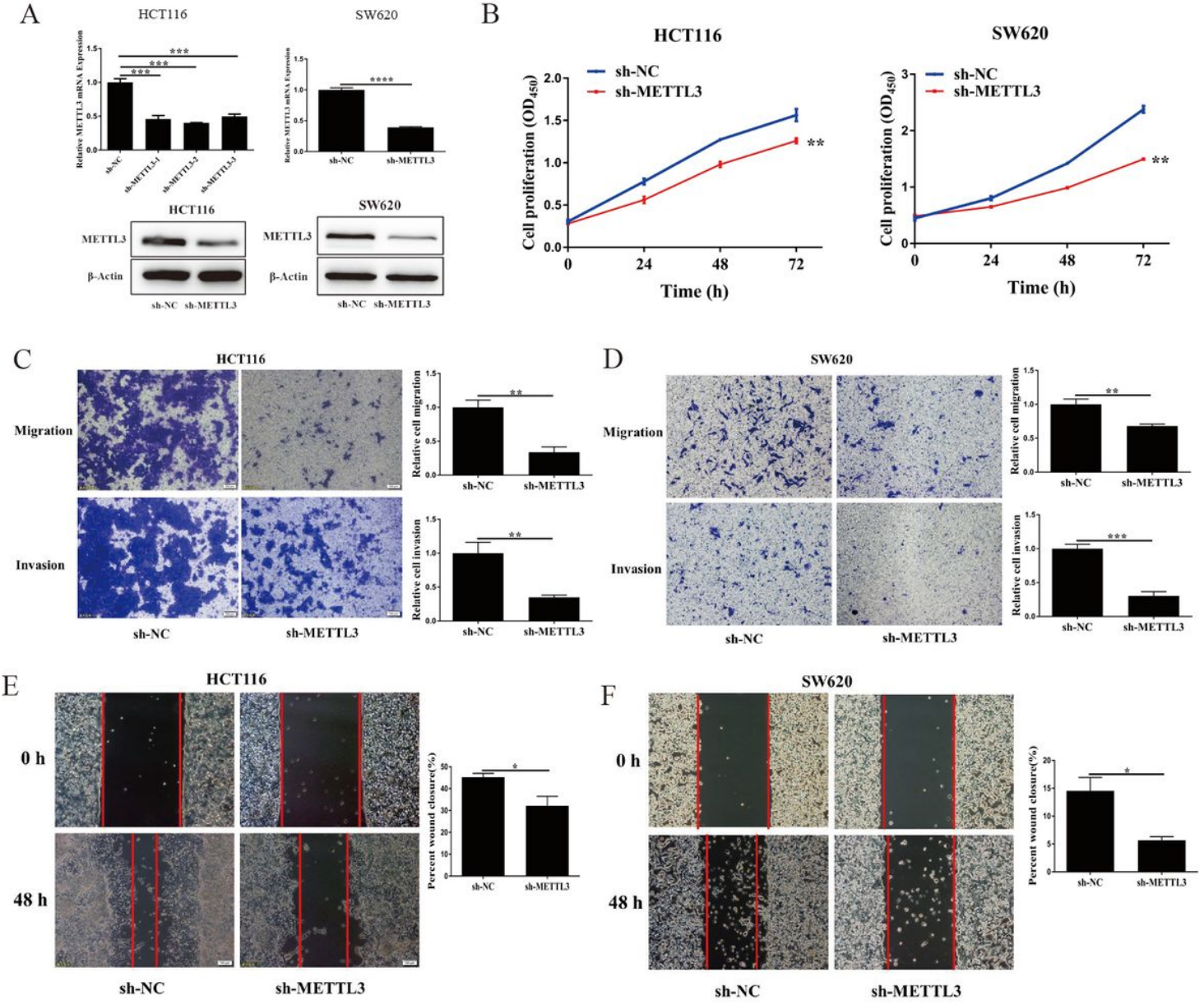

Figure 3

METTL3 drives CRC proliferation and invasion. (a) The expression of METTL3 in HCT116 and SW620 cells with METTL3 knockdown were measured; (b) The proliferation of HCT116 and SW620 cells were measured after METTL3 knockdown; Transwell assays were performed with METTL3 knockdown in HCT116 cell (c), and SW620 cell (d); Wound healing assay were performed with METTL3 knockdown in HCT116 cell (e), and SW620 cell (f). Data were presented as means ±SD. *P < 0.05, **P < 0.01, ***P < 0.001.

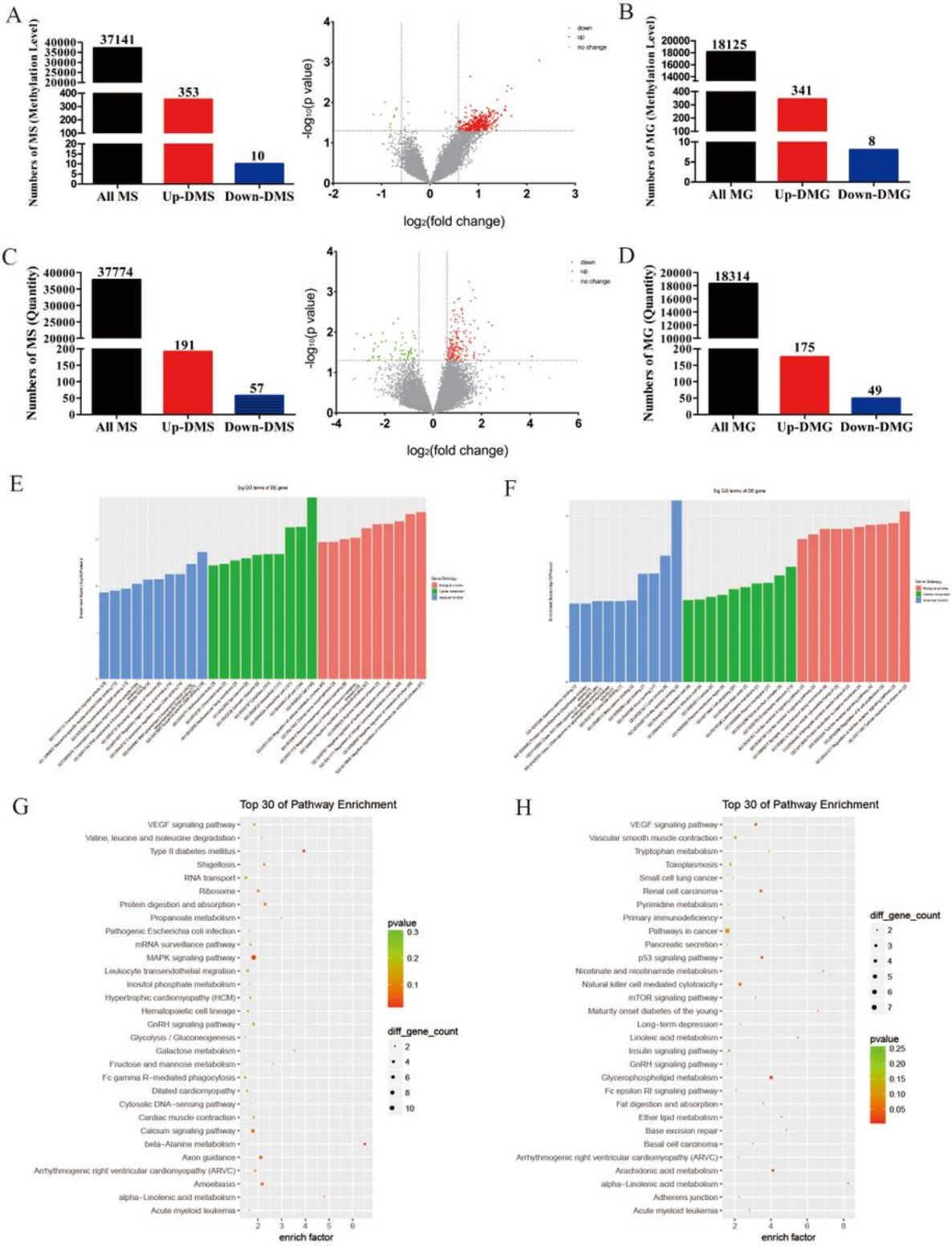

Figure 4

The analysis of the epitranscriptomic microarray. The analysis of differentially m6A methylated sites (a) and differentially m6A methylated genes (b) in the m6A methylation level; The analysis of differentially m6A methylated sites (c) and differentially m6A methylated genes (d) in the m6A quantity level; (e-f) The analysis of GO in m6A methylation level and m6A quantity level; (g-h) The analysis of KEGG in m6A methylation level and m6A quantity level.

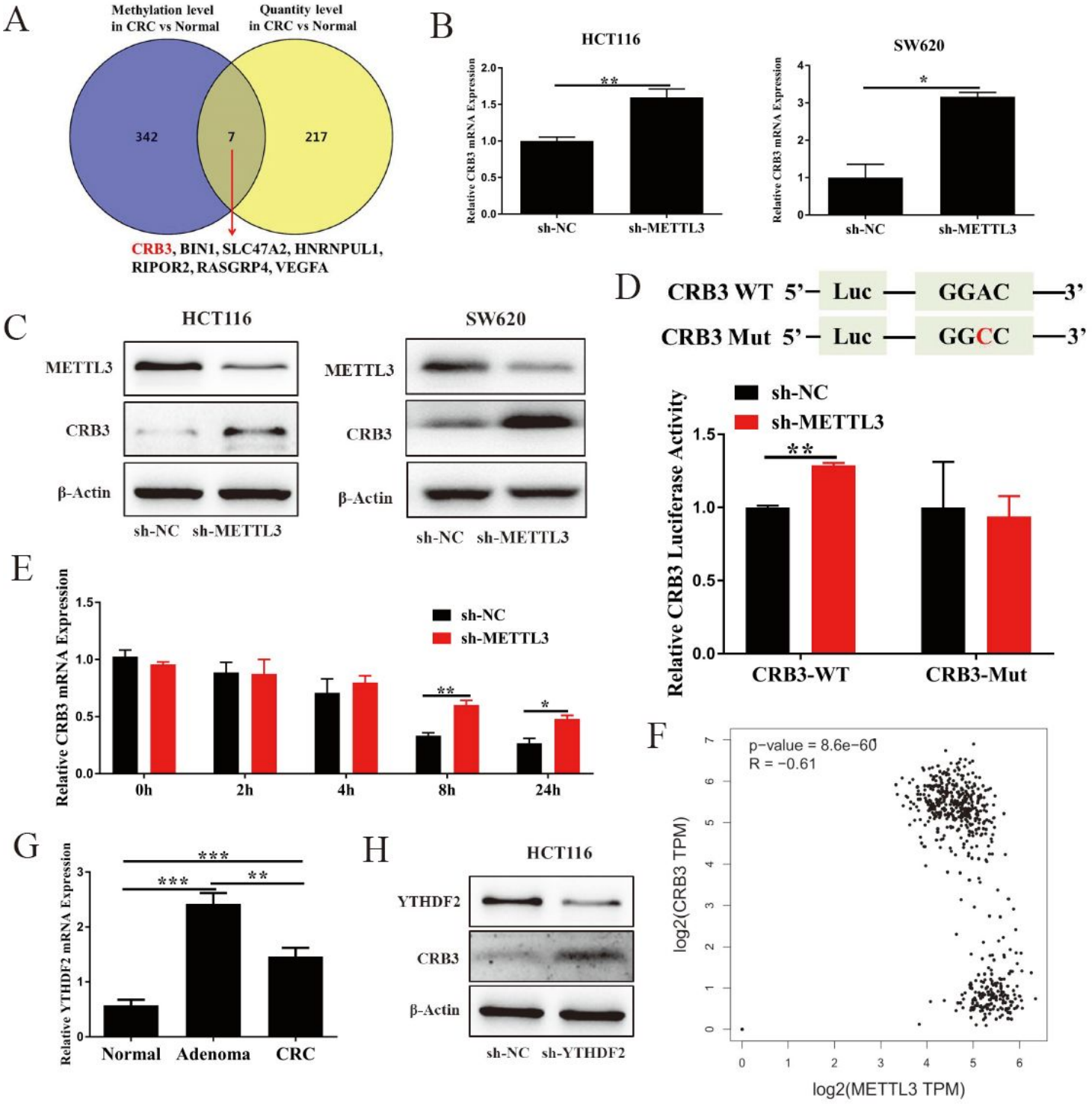

Figure 5

CRB3 was regulated by METTL3-mediated m6A modification. (a) Overlapping DMG between the m6A methylation level and quantity level were filtered by a Venn diagram; (b) The CRB3 mRNA level was measured after METTL3 knockdown; (c) The CRB3 protein level was measured after METTL3 knockdown; (d) Luciferase reporters were performed to determine the effect of m6A modification on CRB3 expression; (e) The CRB3 mRNA expression were detected with or without treatment of actinomycin D at indicated times; (f) Correlation between METTL3 and CRB3 expression in TCGA database for COAD

was analyzed; (g) The YTHDF2 mRNA level was measured in both adenoma and CRC; (h) The CRB3 protein level was measured after YTHDF2 knockdown. Data were presented as means ± SD. *P < 0.05, **P < 0.01, ***P < 0.001.

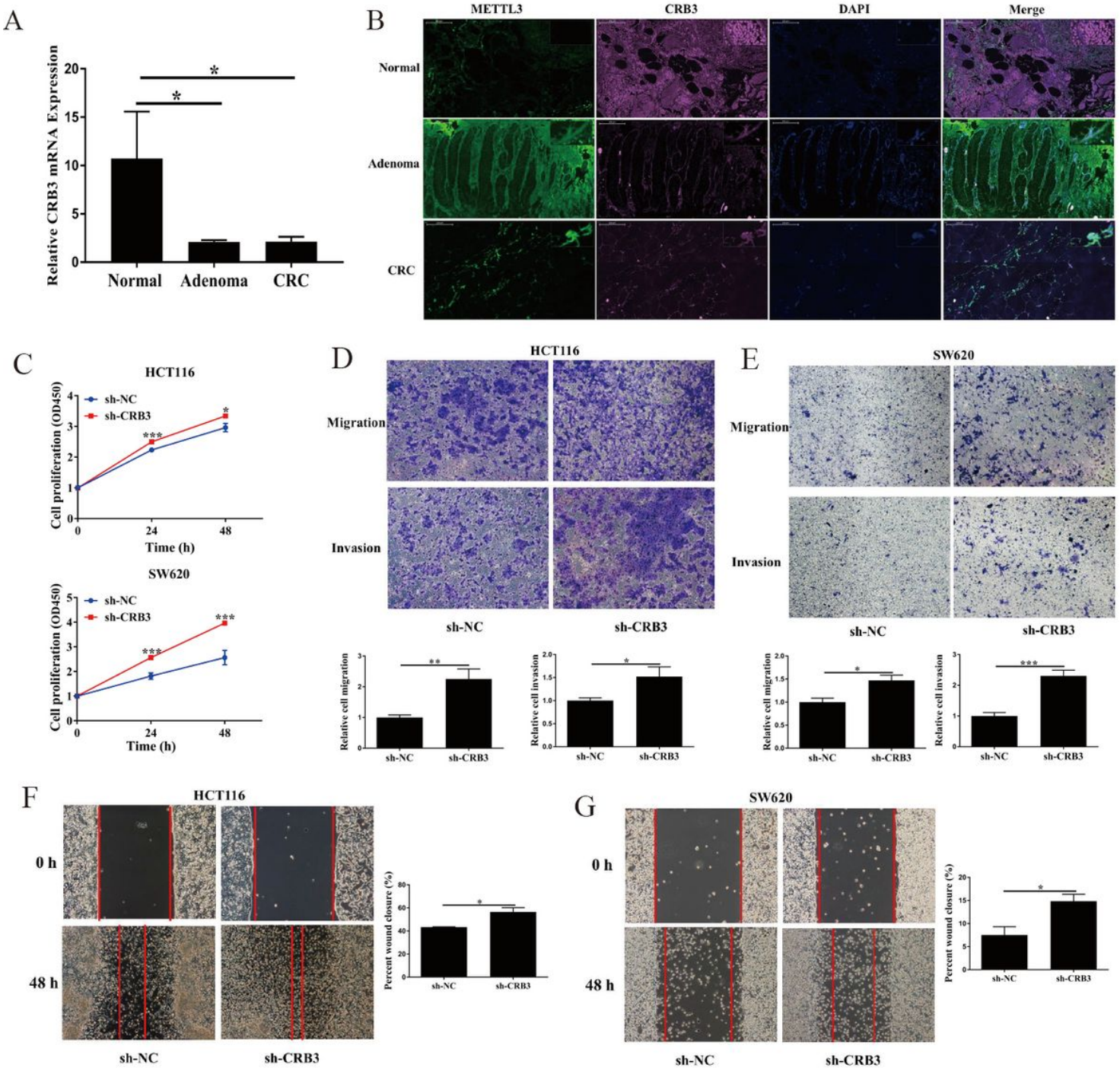

Figure 6

CRB3 inhibited CRC proliferation and invasion. CRB3 expression in both adenoma and CRC was assayed by qPCR (a), and Immunofluorescence (b); (c) The proliferation of HCT116 and SW620 cells were measured after CRB3 knockdown; Transwell assays were performed with CRB3 knockdown in HCT116 cell (d), and SW620 cell (e); Wound healing assay were performed with CRB3 knockdown in HCT116 cell (f), and SW620 cell (g). Data were presented as means ± SD. *P < 0.05, **P < 0.01, ***P < 0.001.

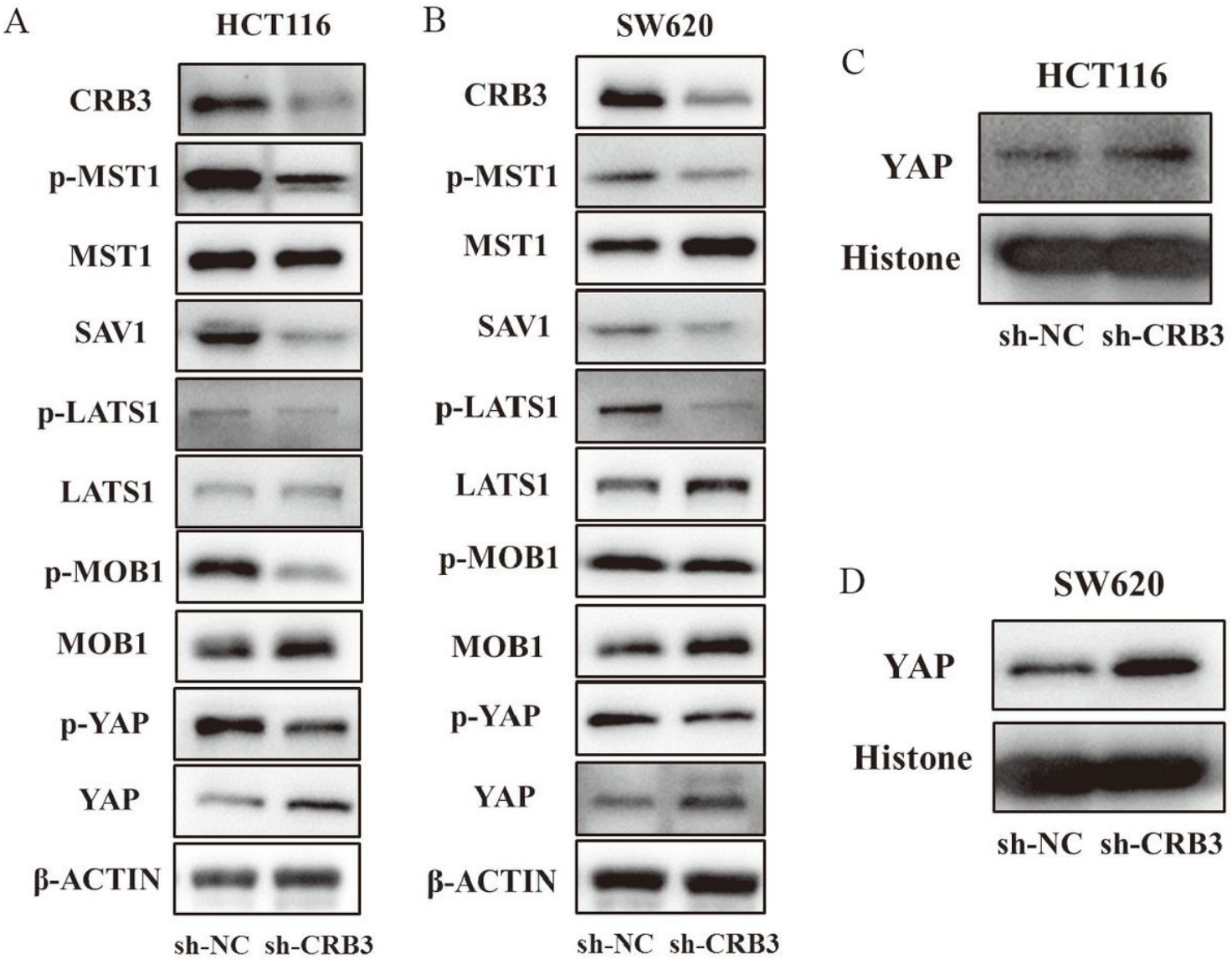

Figure 7

CRB3 inhibited CRC progression by regulating Hippo pathway. Hippo pathway was detected after CRB3 knockdown in HCT116 cell (a), and SW620 cell (b); YAP protein level was detected after CRB3 knockdown in the nucleus of HCT116 cell (c), and SW620 cell (d).

Supplementary Files

This is a list of supplementary files associated with this preprint. Click to download.

- Additionalfile1FigureS1.tif
- Additionalfile2FigureS2.tif
- Additionalfile3.docx
- Additionalfile4.xlsx

- Additionalfile5.xlsx